

Global structure of Bose-Einstein condensates at high rotation: Beyond the lowest Landau level description

Gentaro Watanabe^{a,b,c} and C. J. Pethick^b

^aDepartment of Physics, University of Tokyo, Tokyo 113-0033, Japan

^bNORDITA, Blegdamsvej 17, DK-2100 Copenhagen, Denmark

^cComputational Astrophysics Laboratory, RIKEN, Saitama 351-0198, Japan

(Dated: April 14, 2024)

We study the global density profile of a rapidly rotating Bose-Einstein condensate in a harmonic trap with transverse frequency ω_\perp . By introducing an additional variational degree of freedom to the lowest Landau level wave function, we demonstrate that with increasing strength of the interparticle interaction, the global density profile changes from a Gaussian to the inverted parabolic one characteristic of Thomas-Fermi theory. The criterion for the lowest Landau level wave function to be a good approximation for the global structure is that the mean field energy be small compared with $\hbar\omega_\perp = N_v$, where N_v is the number of vortices in the cloud. This condition is more stringent than the requirement that the mean field energy be small compared with $\hbar\omega_\perp$ which is necessary for the lowest Landau level wave function to be a good approximation to the local structure. Our results show that the lowest Landau level wave function is inappropriate for the global structure of the system realized in recent experiments even though this wave function can describe the local structure well.

PACS numbers: 03.75.Hh, 05.30.Jp, 67.40.Vs, 67.40.Db

Quantized vorticity and vortex lines are characteristic features of superfluids [1, 2] and since the first observation of a vortex in a Bose-Einstein condensed atomic gas [3], many beautiful experiments have been performed to observe vortex lines and vortex lattices in these systems [5, 6, 7]. One fundamental question is how condensates behave when the vortex core size become comparable to the spacing between vortices. Such conditions have not been achieved for superfluid liquid helium-4, but they have been for atomic gases in harmonic traps. Ho noted that the Hamiltonian for a rotating gas in a harmonic trap is similar to that for charged particles in a magnetic field, and he argued that for rotational angular velocities just below the radial trap frequency ω_\perp all particles would condense into the lowest Landau level (LLL) of the rotational motion [9]. Motivated by this suggestion, Schweikhard et al. have recently achieved rotational angular velocities in excess of 0.99 ω_\perp , at which the cloud contains a number of vortices of order one hundred [10]. The frontiers of experiments have reached the so-called "mean-field quantum Hall" regime where the $\hbar\omega_\perp$ is large compared with the interaction energy, that is $\hbar\omega_\perp \gg g n$, where n is the particle density and $g = 4\pi\hbar^2 a/m$ is the effective two-body interaction, m being the particles mass and a the scattering length.

Employing a quantum Hall like wave function, which contains only components in the lowest Landau levels, Ho predicted that the smoothed density profile of a trapped cloud would be Gaussian. To understand the difference between the conventional approach to slowly-rotating condensates and rapidly-rotating ones, the authors of Ref. [11] (see also Ref. [12]) adopted a more general wave function consisting of the product of a slowly varying envelope function, which describes the global structure of the cloud and a rapidly varying one which describes the

properties of individual vortices. They concluded that the density profile would have the inverted parabolic form characteristic of Thomas-Fermi theory, rather than the Gaussian one.

In the present paper, we consider the properties of a rotating cloud in a potential $V(r) = \frac{1}{2}m\omega_\perp^2 r^2$, using a trial wave function which is a generalization of the lowest Landau level one. We find that the global structure of the cloud is of the Thomas-Fermi form provided $\hbar\omega_\perp \gg N_v$, where N_v is the number of vortices within the cloud. For simplicity, we confine ourselves mainly to the two-dimensional problem in this paper.

We shall use for the wave function of the condensed state the expression

$$\psi(r) = N^{-1/2} h(r) \psi_{LLL}^{N=2}(r); \quad (1)$$

where N is the number of particles in the condensate and the lowest Landau level wave function ψ_{LLL} has the general form (i.e., quantum Hall like wave function) as in Ref. [9]:

$$\psi_{LLL}(r) = A e^{-r^2/2a_\perp^2} \prod_{i=1}^N (\zeta - \zeta_i); \quad (2)$$

where $\zeta = x + iy$, ζ_i are the vortex positions, $a_\perp = (\hbar/m\omega_\perp)^{1/2}$ and A is the normalization constant. The function h which changes the density profile from the form predicted by the lowest Landau level calculation, is real, and varies slowly on the scale of the intervortex separation. In the lowest Landau level wave function, the positions of vortices determine the density distribution, apart from an overall multiplicative constant, and the introduction of the modulating function allows us to break this requirement. The normalization condition for

the wave function is $\int d^2r h^2 j_{LLL}^2 = 1$. The normalization condition for j_{LLL} is arbitrary, but for definiteness we shall make the choice $\int d^2r j_{LLL}^2 = 1$.

The energy per particle of the condensate in the rotating frame is given by $E^0 = E - \Omega L_z$, where E is the energy in the non-rotating frame and L_z is the expectation value of the angular momentum per particle about the axis of rotation. Following Ho [9], we write this in the form

$$E^0 = \left(\int d^2r \left[\frac{m}{2} \left(\frac{h}{m} \right)^2 \left(\frac{dr}{dr} \right)^2 + \frac{g_{2D}}{2} j_{LLL}^2 \right] \right) / \int d^2r h^2 j_{LLL}^2; \quad (3)$$

where $\int d^2r = \int d^2r / 2\pi$.

An important observation is that even if the spatial variations of h are of order unity over the cloud, the admixture of excited Landau levels in the wave function (1) is of order $a_2^2 dh/dr \approx R^{-1} = N_v^{-1/2}$ relative to the LLL contribution [13]. Here R is the radial extent of the cloud and $N_v = R^2/a_2^2$ is the number of vortices in the cloud. From this one can show that, apart from corrections of order $h(\partial/\partial r) = N_v$, for the wave function (1), one finds

$$E^0 = h + \int d^2r h j_{LLL}^2 \left(\frac{h^2}{2m} \frac{dh}{dr} \right)^2 + h \left(\frac{r^2}{a_2^2} h^2 + \frac{bg_{2D}}{2} h j_{LLL}^2 \right) h^4; \quad (4)$$

Here g_{2D} is the effective coupling parameter in two dimensions and $b \int d^2r h j_{LLL}^4 = \int d^2r h j_{LLL}^2$ is a factor of order unity describing the renormalization of the effective interaction due to the rapid density variations on the scale of the vortex separation [11, 12, 14].

If the wave function is uniform in the direction of the axis of rotation, $g_{2D} = N g / Z$, where Z is the axial extent of the cloud, while if the wave function for motion in the direction of the rotation axis corresponds to the ground state of a particle in a harmonic oscillator potential with frequency ω_z , $g_{2D} = N g / (2 a_z)$, where $a_z = (\hbar/m \omega_z)^{1/2}$ [15]. Since the terms in braces in Eq. (4) vary slowly in space, we may obtain a good approximation to the energy by making the averaged vortex approximation as in Ref. [9]. Like Ho, we shall in this paper assume that the number of vortices per unit area is uniform. If the vortex density is nonuniform, this will increase the interaction energy, which for a uniform system is a minimum for a regular triangular lattice. For such a uniform array of vortices, one finds

$$h j_{LLL}^2 \approx \frac{1}{2} e^{r^2/a_2^2}; \quad (5)$$

Here $h :: i$ denotes an average over an area of linear size large compared with the vortex separation but small compared with a_2 . The width a_2 is given by $1/a_2^2 =$

$1/a_2^2 = n_v$, where n_v is the average vortex density in the plane perpendicular to the rotation axis [9].

The first term in braces in Eq. (4) represents the extra kinetic energy associated with admixture of excited Landau levels. It scales with the radius of the system in the same way as the interaction energy. If $g_{2D} \approx \hbar^2/m$, the first term suppresses spatial variations of h , and the solution is $h \approx 1$, and the wave function reduces to the LLL one. The condition for the LLL wave function to be a good approximation may also be written as $N a_2^2 \approx 1$. In current experiments $N a_2^2$ is of order 10-100, so this condition is strongly violated. In the opposite limit, $g_{2D} \approx \hbar^2/m$, the extra kinetic energy is unimportant, and the optimal density profile is obtained by minimizing the second and third terms in the integrand, which results in a Thomas-Fermi density profile. Another way to express the criterion for validity of the LLL approximation is that the interaction energy per particle, gn , be small compared with $\hbar \omega_z = N \omega_z$, rather than the condition $\hbar \omega_z$ which has generally been assumed in earlier work.

To obtain quantitative results we perform a variational calculation with a trial function that interpolates between the Gaussian and Thomas-Fermi forms. We exploit the fact that $\lim_{t \rightarrow 1} (1 - t) = e^{-t}$ as Fetter did in calculations for non-rotating clouds [16]. Thus we take

$$h(r) = A_h \left(1 - \frac{r^2}{L^2} \right)^2 e^{r^2/2L^2}; \quad (6)$$

for $0 \leq r < L$ and otherwise $h = 0$. The normalization factor A_h is given by $A_h^2 = (\pi^2/L^2)(1 + 1/2)$. The number of particles per unit area, divided by N , is given by $\langle r \rangle = \int d^2r h j_{LLL}^2$ with the above expression (6) for h can describe both Gaussian form ($L \gg a_2$) and the Thomas-Fermi one ($L \approx a_2$). Hereafter, we shall refer to the expression (6) for h as the Gaussian-Thomas-Fermi (G-TF) form.

Substituting Eq. (6) into Eq. (4), we obtain the energy E_{G-TF}^0 for the Gaussian-TF modulation

$$E_{G-TF}^0 = h + \frac{h^2}{2} a_2^2 \left(\frac{1}{L^2} + \frac{1}{1} \right) \frac{2}{2} + \frac{L^2}{2} + \frac{L^2}{2} + h \left(\frac{r^2}{a_2^2} h^2 + \frac{bg_{2D}}{2} \frac{1}{L^2} \left(\frac{1}{2} + 1 \right) \right); \quad (7)$$

Minimizing E_{G-TF}^0 with respect to L and a_2 , we obtain the following expressions for these two quantities:

$$L^2 = a_2^2 \left(1 + \frac{1}{2} \right) \frac{1}{1} \left(\frac{1}{2} + 2 \right) \frac{1}{1} + \frac{(1/2)^2}{(2/2 + 1)}; \quad (8)$$

$$\frac{1}{2} = 1 + \frac{2}{L^2} \frac{1}{L^2}; \quad (9)$$

where

$$\frac{m bg_{2D}}{2 \hbar^2}; \quad (10)$$

is a dimensionless parameter determining the strength of interparticle interactions.

Then we minimize E_{G-TF}^0 with respect to α . The optimal value of α is determined by the quartic equation

$$\begin{aligned} &= \frac{1}{2}(1+4\kappa)^2 + \frac{1}{2} \frac{(1+4\kappa)^2 + 8}{(1+4\kappa)^2 + 8} \frac{3}{2} [(1+4\kappa)^2 + 8]^{\frac{1}{2}} \\ &+ \frac{1}{2} 4 \frac{(1+4\kappa)^2 + 8}{(1+4\kappa)^2 + 8} + 3 \frac{2}{2} [(1+4\kappa)^2 + 8]^{\frac{1}{2}} + \frac{2(1+2\kappa)^2 + 2(1+4\kappa)^2 + 8}{(1+4\kappa)^2 + 8} \frac{3}{2} \frac{1}{5} ; \end{aligned} \quad (11)$$

since the three other solutions give negative or complex values of α . In the limits of weak ($\kappa \rightarrow 0$) and strong interaction ($\kappa \rightarrow \infty$) the above solution behaves as

$$\alpha = \frac{1}{2}(1+4\kappa)^2 ; \text{ and} \quad (12)$$

$$\alpha = 1 + \frac{3}{2\kappa} \frac{1}{\kappa} + O(\frac{1}{\kappa^2}) \quad (\frac{1}{\kappa} \rightarrow 0) : \quad (13)$$

Observe that α does not depend on κ .

The shape index α given by Eq. (11) is plotted in Fig. 1, and it decreases from infinity in the absence of interaction to unity as the strength of the interaction (κ) increases from zero to infinity. This means that the density profile of the cloud changes from a Gaussian to an inverted parabola due to the interaction. Without the minimization with respect to α , we can describe the cloud with an assumption on the shape of the density profile corresponding to the given value of the shape index. For the parameters L and μ , we can use the expressions of Eqs. (8) and (9). If we take $\kappa \rightarrow 1$, we reproduce a Gaussian density profile as in the case without the modulating function, but its width is optimized.

Now we compare the results of the following two cases: the Gaussian-TF profile with an optimized value of α and the Gaussian profile with $\alpha = 1$, and discuss the situation relevant to the experiments. For definiteness, we write the energy for the Gaussian profile as E_G^0 , which can be obtained by taking $\kappa \rightarrow 1$ in Eq. (7). Relative energy differences $(E_{G-TF}^0 - E_G^0) = (E_G^0 - \hbar^2 \mu)$ between the Gaussian-TF and Gaussian cases are shown in Fig. 2. In the limit $\kappa \rightarrow 1$, the leading terms are

$$E_G^0 \approx \hbar^2 \mu + \frac{\hbar^2 \mu}{2} \frac{1}{\kappa} \frac{1}{\kappa} ; \quad (14)$$

$$E_{G-TF}^0 \approx \hbar^2 \mu + \frac{4}{3} \hbar^2 \mu \frac{1}{\kappa} \frac{1}{\kappa} ; \quad (15)$$

Thus, in this limit, the relative energy difference $(E_{G-TF}^0 - E_G^0) = (E_G^0 - \hbar^2 \mu)$ converges to $(\frac{4}{3} - 1) = \frac{1}{3} \approx 0.33$ irrespective of the value of κ (see Fig. 2). This result shows us that the density profile can change

markedly even though the energy reduction is less than 6%.

We now consider the system realized in Ref. [10] rotating at $\omega = 0.99 \omega_c$, which is typical of the highest angular velocities achieved so far. If we assume that the density is uniform in the axial direction, we get $\mu = (2N a) \hbar \omega_c > 52$ using the relation $g_{2D} = gN = \hbar^2 \mu$ and the experimental data $N a \hbar \omega_c > 26$ given in Ref. [10]. If we assume a Gaussian density profile in this direction instead of the uniform one, we obtain $\mu = 2N a \hbar \omega_c = (2 a_z) \hbar \omega_c > 1.4 \times 10^5$ using $g_{2D} = gN = \hbar^2 \mu$, $a_z = 2.5 \times 10^{-8} \text{ m}$, $N = 1.5 \times 10^8$ at $\omega = 0.989 \omega_c$, and $a = 5.6 \text{ nm}$ for the triplet state of ^{87}Rb . Thus we conclude that the typical value of the parameter relevant to the experiments of Ref. [10] is of order 10^2 .

In Fig. 3, we plot the global profile for the number of particles per unit area $\langle n \rangle = \hbar^2 \mu / (2 \pi \hbar^2)$ at $\omega = 0.99 \omega_c$ and $\omega = 100$ for the Gaussian-TF case in addition to those for the two extreme cases of the Gaussian form with

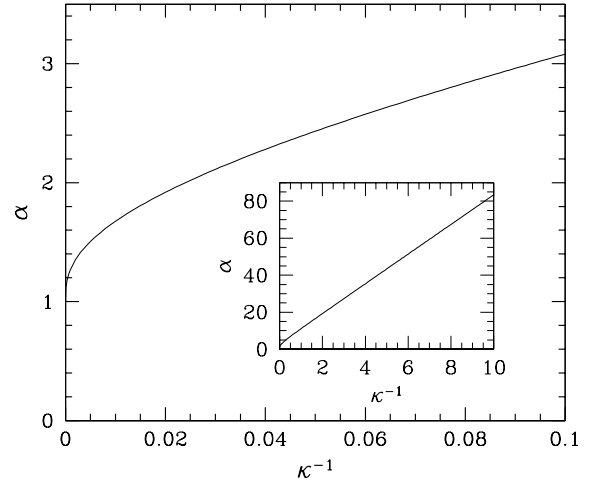


FIG. 1: Shape index α as a function of κ^{-1} covering a range of interaction strengths typical of current experiments ($\kappa \approx 100$). In the inset, α is plotted over a wider range of κ^{-1} to show its asymptotic behavior (12).

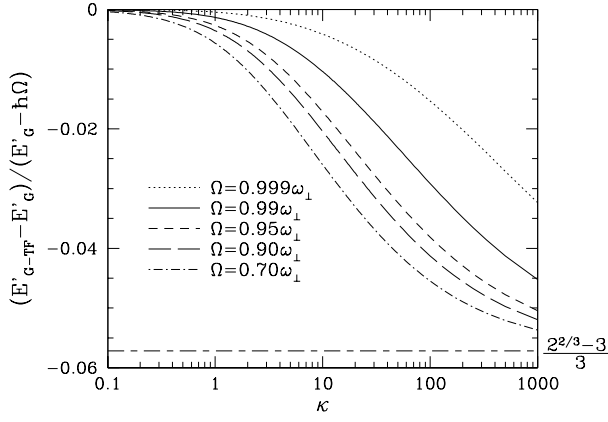


FIG. 2: Difference between the energies E_{G-TF}^0 calculated in the Gaussian-TF case with the optimized ψ given by Eq. (11) and E_G^0 in the Gaussian case with $\psi = 1$, relative to $E_G^0 - \hbar\Omega$. For any value of Ω , the curve converges to $(2^{2/3} - 3)/3 = -0.0572$ in the limit of $\Omega \rightarrow 1$.

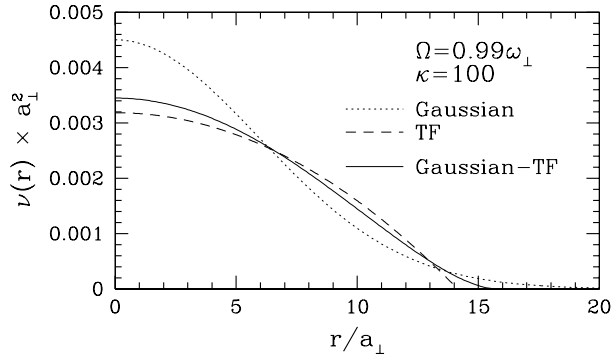


FIG. 3: Global density profile $\nu(r) = \hbar^2 \hbar_{LLL} \int |\psi|^2$ of the cloud for $\Omega = 0.99\omega_\perp$ and $\kappa = 100$. The solid line is obtained for the optimized ψ given by Eq. (11). The dotted line and dashed one are obtained for $\psi = 1$ and $\psi = 1$, respectively.

$\psi = 1$ and the inverted parabolic one labelled as "TF". The latter is obtained by the procedure corresponding to the Thomas-Fermi approximation in the non-rotating case in which we neglect the contribution from the first term in the braces in Eq. (4) [i.e., the second term in Eq. (7)]. As can be seen from the solid line of this figure, the density profile for the Gaussian-TF modulation is closer to the TF case than to the Gaussian one and it can be fitted rather well by an inverted parabola except at the edge of the cloud [17]. From Fig. 2 one can see that the relative energy reduction compared with that for the Gaussian approximation is only $\sim 2.9\%$.

In this paper, we have demonstrated that the global density profile of a rapidly rotating Bose-Einstein condensate is not well described by the lowest Landau level wave function, even though the mean field energy is small compared with $\hbar\Omega$, a condition satisfied in recent experiments. By performing a variational calculation with a trial wave function which includes components in excited Landau levels, we have shown how the density profile changes from a Gaussian to the Thomas-Fermi form as the strength of the interparticle interaction increases. The reduction in the energy resulting from the extra degree of freedom in the wave function is of the order of one per cent. The approach described in this paper may be generalized to time-dependent problems by deriving equations for the evolution of the variational parameters from the condition that the action be stationary.

This work arose as a result of discussions and correspondence with Gordon Baym, to whom we are very grateful. In addition, we thank V. Cheianov for helpful comments. G.W. thanks K. Sato, K. Yasuoka, and T. Ebisuzaki for continuous encouragement and L.M. Jensen, and P. Urkedal for arranging the computer environment. This work was supported by Grants-in-Aid for Scientific Research provided by the Ministry of Education, Culture, Sports, Science and Technology through Research Grant No. 14-7939.

-
- [1] R. J. Donnelly, *Quantized Vortices in Helium II* (Cambridge University Press, Cambridge, 1991).
 - [2] E. B. Sonin, *Rev. Mod. Phys.* **59**, 87 (1987).
 - [3] M. R. Matthews, B. P. Anderson, P. C. Haljan, D. S. Hall, C. E. Wieman, and E. A. Cornell, *Phys. Rev. Lett.* **83**, 2498 (1999).
 - [4] A. L. Fetter and A. A. Svidzinsky, *J. Phys. : Condens. Matter* **13**, R135 (2001).
 - [5] K. W. Madison, F. Chevy, W. Wohlleben, and J. Dalibard, *Phys. Rev. Lett.* **84**, 806 (2000).
 - [6] J. R. Abo-Shaer, C. Raman, J. M. Vogels, and W. Ketterle, *Science* **292**, 476 (2001).
 - [7] P. C. Haljan, I. Coddington, P. Engels, and E. A. Cornell, *Phys. Rev. Lett.* **87**, 210403 (2001).
 - [8] P. Engels, I. Coddington, P. C. Haljan, and E. A. Cornell, *Phys. Rev. Lett.* **89**, 100403 (2002).
 - [9] T.-L. Ho, *Phys. Rev. Lett.* **87**, 060403 (2001).
 - [10] V. Schweikhard, I. Coddington, P. Engels, V. P. Mosenfelder, and E. A. Cornell, *cond-mat/0308582*.
 - [11] G. Baym and C. J. Pethick, *Phys. Rev. A* (in press), (*cond-mat/0308325*).
 - [12] U. R. Fischer and G. Baym, *Phys. Rev. Lett.* **90**, 140402 (2003).
 - [13] This will be demonstrated in detail elsewhere (G. Watanabe and C. J. Pethick, in preparation).
 - [14] J. Sinova, C. B. Hanna, and A. H. MacDonald, *Phys. Rev. Lett.* **89**, 030403 (2002).
 - [15] A. L. Fetter, *Phys. Rev. A* **68**, 063617 (2003).
 - [16] A. L. Fetter, *J. Low Temp. Phys.* **106**, 643 (1997).
 - [17] In the region $r < 10a_\perp$, the solid curve in Fig. 3 can be fitted quite well by the inverted parabola $\nu(r)a_\perp^2 = 0.00343 - 2.1 \times 10^{-5} (r/a_\perp)^2$.